FEBS Letters 374 (1995) 62–68 FEBS 16149

Specific RNA cleavages induced by manganese ions

Jan Wrzesinski, Daniel Michałowski, Jerzy Ciesiołka, Wlodzimierz J. Krzyżosiak*

Institute of Bioorganic Chemistry, Polish Academy of Sciences, ul. Noskowskiego 12, 61-704 Poznan, Poland

Received 4 August 1995

Abstract The specificity and efficiency of manganese ion-induced RNA hydrolysis was studied with several tRNA molecules. In case of yeast $tRNA^{Phe}$, the main cleavage occurs at p16 and minor cuts at p17–18, p20–21, p34 and p36–37. The major Mn(II)-induced cut in yeast elongator $tRNA^{Met}$ is also located in the D-loop at p16 and it is stronger than that observed in $tRNA^{Phe}$. In initiator $tRNA^{Met}$ from yeast two strong Mn(II) cleavages of equal intensity occur at p16 and p17. This is in contrast with single, much weaker cuts induced in the D-loop of that tRNA by Mg(II), Eu(III) and Pb(II) ions. Interestingly, in case of yeast $tRNA^{Glu}$ the main cleavage caused by Mn(II), Mg(II) and Pb(II) ions occurs in the anticodon loop. The involvement of hypermodified base mnm^5s^2U in this cleavage was ruled out based on results obtained with in vitro transcript of yeast $tRNA^{Glu}$ anticodon arm. Mutation of a single base A37G in the anticodon loop of the transcript drastically reduced the specificity of Mn(II)-induced hydrolysis.

Key words: Manganese; Ion-induced hydrolysis; tRNA; Transcription, in vitro; tRNA AC-arm mutants

1. Introduction

Interaction of divalent metal ions, in particular Mg(II), with tRNA is essential for stabilization of the tRNA tertiary structure [1]. The best-characterized Mg(II) ions bind mainly to the sugar-phosphate backbone neutralizing negative charges and form weak metal ion binding sites ($K_d \sim 10^{-3}$ M). Moreover, in the tRNA tertiary structure several strong metal ion binding sites exist with $K_d \sim 10^{-6}$ M [2]. Location of some strong metal ion binding sites in yeast $tRNA^{Phe}$ structure has been established with the atomic resolution for Sm(III), Lu(III), Mg(II), Mn(II), Co(II) Pb(II), Zn(II) ions [3–9]. Some of the ions, as Pb(II), Eu(III) and Mg(II), located in their strong binding sites cleave efficiently the D-loop of yeast $tRNA^{Phe}$ in solution [10–13]. The tRNA fragments obtained contain 2′,3′-cyclic phosphate and 5′-hydroxyl termini. The crystallographic studies of yeast $tRNA^{Phe}$ have shown that specific metal ions involved in the D-loop cleavage are coordinated in the region between the D- and T-loops [3–9]. The metal ion-induced RNA hydrolysis reaction has been exploited in three ways: (1) for probing strong metal binding sites in natural tRNAs in solution [11–16]; (2) as a sensitive probe to monitor proper tertiary folding of tRNA mutants or variants [17–21]; and (3) for structure probing of other RNAs and RNA–protein complexes [22–26].

In order to expand the set of RNA structure probing reagents we have analysed the tRNA hydrolysis reactions induced by manganese ions in yeast $tRNA^{Phe}$, in a pair of methionine-specific tRNAs as well as in yeast glutamic acid accepting tRNA which is strongly cleaved in the anticodon loop. Also, the specificity of Mn(II) ion-induced hydrolysis in tRNA fragment containing the yeast $tRNA^{Glu}$ anticodon arm has been investigated.

2. Materials and methods

2.1. Isolation of yeast tRNA

Yeast $tRNA^{Phe}$, $tRNA^{Glu}$ as well as initiator and elongator $tRNA^{Met}$ of specific acceptance 1200–1400 pmol/A_{260} unit were prepared from crude bakers yeast tRNA by standard column chromatography procedures including benzoylated DEAE-cellulose and Sepharose 4B. Final purification was done by HPLC on TSK-gel DEAE-2SW (Toyo-Soda) column. For $tRNA^{Glu}$ purification TSK gel 5PW column (Toyo-Soda) was used.

2.2. Preparation of the yeast $tRNA^{Glu}$ anticodon arm

The $tRNA^{Glu}$ anticodon arm and its U37G mutant were synthesized using T7 RNA polymerase and synthetic DNA templates following the procedure described by Milligan et al. [27]. DNA oligomers: (1) 5′-TAATACGACTCACTATA-3′; (2) 5′-GGGCCACGGTGAAAGCG-(T/C)GACCCTATAGTGAGTCGTCGTATTA were synthesized on an Applied Biosystems 392 DNA/RNA synthesizer. The oligomers were deprotected and purified on OPC column (Applied Biosystems), according to manufacturer's recommendation. The DNA oligomers were hybridized in the buffer containing 10 mM Tris-HCl pH 8.0, 1 mM EDTA by heating at 90°C for 3 min and rapid cooling on ice. The transcription reaction was carried out in 40 mM Tris-HCl pH 8.0, 8 mM $MgCl_2$, 2 mM spermidine, 20 mM DTT, 50 mM NaCl, 1 mM NTPs, 3 mM guanosine, 200 nM DNA template and 3000 U/ml T7 RNA polymerase for 3 h at 37°C. The transcription reaction was stopped by phenol extraction, RNA precipitated with ethanol, the pellet collected by centrifugation, dissolved in water and used for labeling without purification.

2.3. Labeling of tRNA

All studied native tRNAs were 5′-end labeled by dephosphorylation with bacterial alkaline phosphatase and phosphorylated with [γ-^{32}P]ATP (5000 Ci/mmol; Amersham) and polynucleotide kinase. The RNA transcripts were phosphorylated directly. The 3′-end labeling was done on the tRNA deprived of its 3′-terminal sequence by phosphodiesterase treatment. Reconstruction of the natural CCA end was achieved with CTP, [α-^{32}P]ATP (400 Ci/mmol; Amersham) and tRNA nucleotidyltransferase. After labeling tRNA was purified on denaturing 12.5% polyacrylamide gel, located by autoradiography, excised and eluted from the gel with 0.3 M potassium acetate of pH 5.1, 1 mM EDTA and 0.1% SDS. Then the eluted tRNA was ethanol precipitated, dissolved in water and stored at −20°C before use.

2.4. Metal ion induced cleavage

The labeled tRNAs or yeast $tRNA^{Glu}$ anticodon arm variants obtained from in vitro transcription were supplemented with the corresponding unlabeled RNA to obtain final concentration of 8 mM in 40 mM NaCl and 10 mM Tris-HCl buffer. Prior to reaction the standard denaturation/renaturation procedure was applied. RNA was heated to 55°C and then slowly cooled to 37°C in the presence of 0.1 mM EDTA. The pH of the buffers, concentrations of manganese, magnesium and lead ions used and other reaction parameters are specified in the legends to figures. All reactions were stopped by addition of 8 M urea/dyes with

*Corresponding author. Fax: (48) (61) 52-0532.

SSDI 0014-5793(95)01077-7

20 mM EDTA and directly loaded on a 15% polyacrylamide gel. After electrophoresis, autoradiography was at −20°C.

2.5. Analysis of reaction products

In order to assign cleavage sites the products of Mn(II)-induced hydrolysis were compared to the products of alkaline degradation and limited T_1 nuclease digestion of the same tRNA. Alkaline hydrolysis ladder was generated by incubation of tRNA solution together with 1/5 volume of formamide in boiling water for 10 min. Partial T_1 nuclease digestion of tRNA was performed in denaturing conditions (50 mM sodium citrate pH 4.5, 7 M urea) with 0.1 unit of the enzyme by incubating the reaction mixture for 10 min at 50°C.

3. Results

3.1. Time dependence of hydrolysis

The progress of yeast $tRNA^{Phe}$ reaction with Mn(II) ions as a function of time is shown in Fig. 1A. It is seen that the reaction is specific and hydrolysis occurs only in the D-loop and in the anticodon loop. After 8 h of reaction almost 50% of the tRNA molecule undergoes fragmentation. The main cleavage site is located at p16 in the D-loop and several weak cuts appear at p17–18, p20 and p21 in the D-loop as well as at p34, p36–37 in the anticodon loop. The pattern of Mn(II)-induced hydrolysis in $tRNA^{Phe}$ resembles that described previously for Mg(II) ions [15]

3.2. Mn(II) concentration dependence

The rate of yeast $tRNA^{Phe}$ cleavage increases with concentration of Mn(II) ions (Fig. 1B). This rate increase is approximately linear in the Mn(II) concentration range of 0.3–10 mM, however, at 30 mM Mn(II) ions there is no significant acceleration of the cleavage rate. The quantitative analysis has been performed with 5′-end labeled tRNA by counting radioactivity present in intact tRNA and in its fragments (data not shown). This plateau effect is most likely due to saturation of the Mn(II) binding site in tRNA from which the D-loop cleavage is induced. It is clear from Fig. 1B, that the specificity of the cuts is unchanged over the whole studied Mn(II) ions concentration range and that all cuts observed are of primary character because the same fragments appear from tRNA labeled at either 5′- or 3′-end (Fig. 1A and B, respectively).

Some metal ions promote tRNA precipitation from the solution [12,28] and this effect interferes with quantitative evaluation of the cleavages induced. Analysis of yeast $tRNA^{Phe}$ precipitation by Mn(II) ions shows (data not presented) that only a small fraction of tRNA is precipitated from solution after 10 h of the reaction. This fraction is 3% at 1 mM Mn(II) and reaches 10% at 10 mM Mn(II) ions.

3.3. Comparison of Mn(II) and Mg(II)-induced hydrolysis –pH dependence

The influence of pH on the efficiency and specificity of cleavages induced in yeast $tRNA^{Phe}$ by manganese ions was analyzed at 3 mM and 10 mM Mn(II) in the pH range of 5.0–9.0. The strength of the major cut at p16 increases gradually with pH up to the value of 8.5. At pH 9.0 and 10 mM concentration of Mn(II) ions the reaction loses its specificity and the main cuts

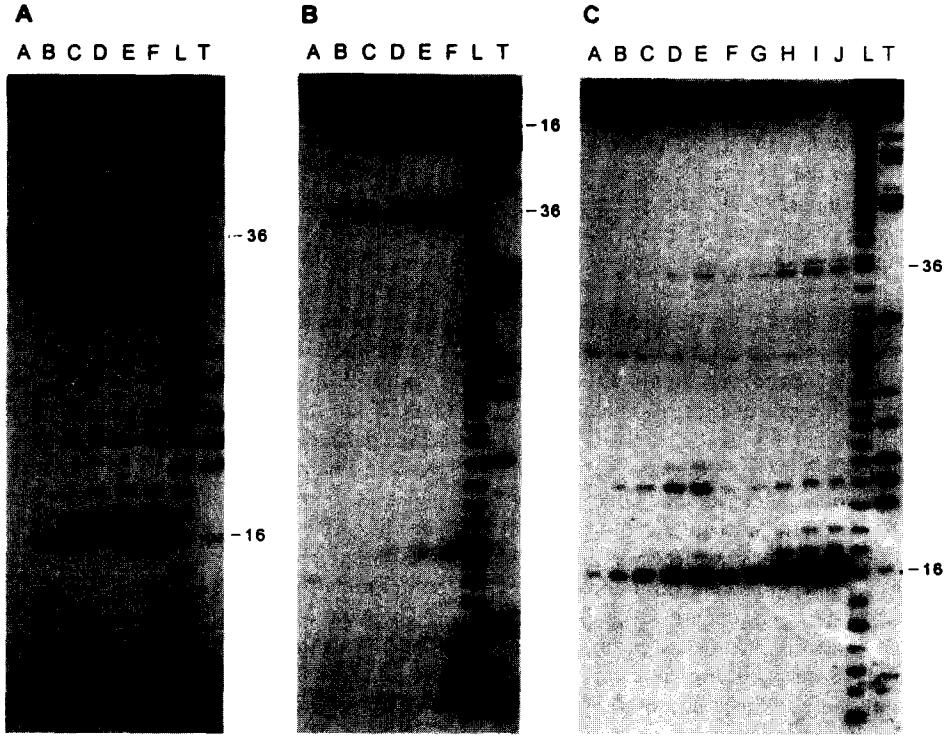

Fig. 1. Mn(II)-induced hydrolysis of 5′-end labeled (A,C) and 3′-end labeled (B) yeast $tRNA^{Phe}$. (A) Time dependence, reaction was carried out at pH 8.0, 10 mM Mn(II) concentration, at 37°C, for various time periods: (B) 0.5 h, (C) 1 h, (D) 2 h, (E) 4 h, and (F) 8 h. Lane A = reaction control, lane L = formamide ladder, lane T = limited hydrolysis by RNase T1. (B) Concentration dependence, reaction was performed at pH 8.0, 37°C for 8 h: lane B = 0.3, lane C = 1, lane D = 3, lane E = 10, lane F = 30 mM Mn(II) concentration. (C) Comparison of Mg(II)- and Mn(II)-induced hydrolysis. Reaction was performed at 37°C, for 8 h at 10 mM Mg(II) and 3 mM Mn(II) concentration at different pH values: lanes A,F = 7.0, lanes B,G = 7.5, lanes C,H = 8.0, lanes D,I = 8.5 and lanes E,J = 9.0 for Mg(II) and Mn(II) ions, respectively. The numbers at the right side indicate the phosphate number.

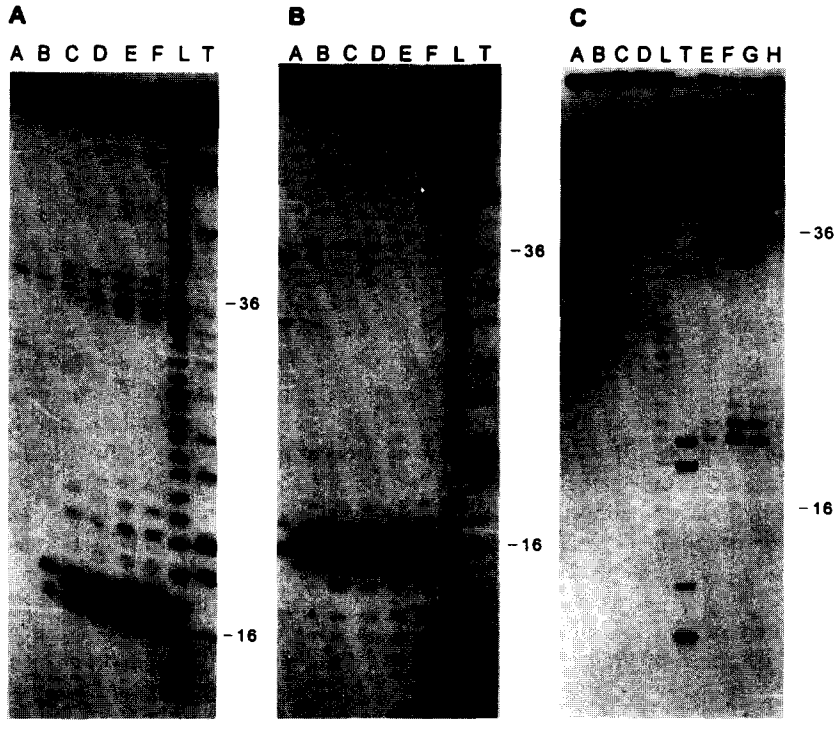

Fig. 2. Mn(II)-induced cleavage of yeast initiator $tRNA^{Met}$ (A), yeast elongator $tRNA^{Met}$ (B) and yeast $tRNA^{Glu}$ (C). Reactions were performed under the same conditions as described in the legend to Fig. 1B. In case of yeast $tRNA^{Glu}$ the Mg(II)- and Mn(II)-induced cleavages are compared (C). Lanes A,H = reaction controls, lanes B,E = 1, lanes C,F = 3, lanes D,G = 10 mM concentration of Mg(II) and Mn(II) ions, respectively. Lane L = formamide ladder, lane T = limited hydrolysis by RNase T_1.

appear on the background of unspecific products of alkaline hydrolysis (data not shown). After 10 h incubation with 10 mM Mn(II) ions 60% of $tRNA^{Phe}$ undergo cleavages at pH 8.5 while only 6% of the tRNA is cleaved at pH 7.0. These changes in reactivity correlate well with the pK_a value of the Mn(II) hydrate determined to be 10.6 [29]. As the pH value of 8.0 guarantees both high rate of cleavages and high specificity of the reaction all further experiments were carried out at this pH.

Results shown in previous sections suggested high similarity of Mn(II)-induced cleavage to that observed for Mg(II) ions. Therefore experiments were performed to compare directly the cleavage effects caused by both kinds of ions. As the cleavage rate was much higher for manganese ions the results shown in Fig. 1C for pH-dependent reactions were obtained with 3 mM Mn(II) and 10 mM Mg(II) ions concentration. Other conditions were identical for both reactions. It turned out that the overall pattern of cleavages induced in yeast $tRNA^{Phe}$ is in fact similar for both ions, however, there are some differences in the reaction rates at the specific sites. The major cut at p16 is 5 times stronger at pH 7.5 and 2.5 times stronger at pH 9.0 in case of Mn(II) ions. The second strongest cut at p20 is, however, 3 times more intense in magnesium-induced hydrolysis reaction at pH 8.5. The ratio of fragment containing nucleotides 1–16 to that containing nucleotides 1–20 is 6.5 for magnesium reaction and 43 for manganese reaction at pH 8.5. These values were obtained from radioactivity counting of excised gel bands. The data shown above suggest that Mn(II) and Mg(II) binding sites in yeast $tRNA^{Phe}$ in solution are highly similar but they are not identical.

3.4. *The Mn(II)-induced hydrolysis of yeast initiator and elongator tRNAMet*

Two different methionine-accepting tRNAs from yeast the initiator and elongator tRNAs were also subjected to manganese-induced hydrolysis. The initiator $tRNA^{Met}$ is cleaved with similar efficiency as yeast $tRNA^{Phe}$ and the most prominent cuts occur at p16 and p17 in the D-loop (Fig. 2A). The hydrolysis induced in this tRNA is, however, significantly more efficient than that caused by other metal ions studied earlier [16]. Also the presence two cuts of nearly equal intensity in the D-loop is the unique feature of manganese ions. The second region involved in hydrolysis is the anticodon loop. It undergoes the Mn(II) ion-induced hydrolysis at almost all phosphates p34–p38. That region is also cleaved by Pb(II), Eu(III) and Mg(II) ions. In the variable region the only reactive phosphates are p46–p48. It was apparent from previous studies [16] that the variable region was completely resistant to Mg(II) ions, but Pb(II) and Eu(III) ions cut that region with low efficiency, comparable to that obtained with Mn(II) ions.

The main Mn(II) ion-induced cleavage appears in elongator $tRNA^{Met}$ at the same position as in yeast tRNAPhe, however, the intensity of $tRNA^{Met}$ cleavage is significantly higher (Fig. 2B). Comparing the Mn(II) and earlier studied Mg(II)-induced hydrolysis of that tRNA [16] some other differences are also observed. In case of Mn(II) ions the cleavages at p17 and p20 in the D-loop are absent and only a single weak cleavage occurs at p37 in the anticodon loop.

3.5. *Mn(II) ion-induced hydrolysis of yeast $tRNA^{Glu}$*

The most interesting is the result obtained with yeast

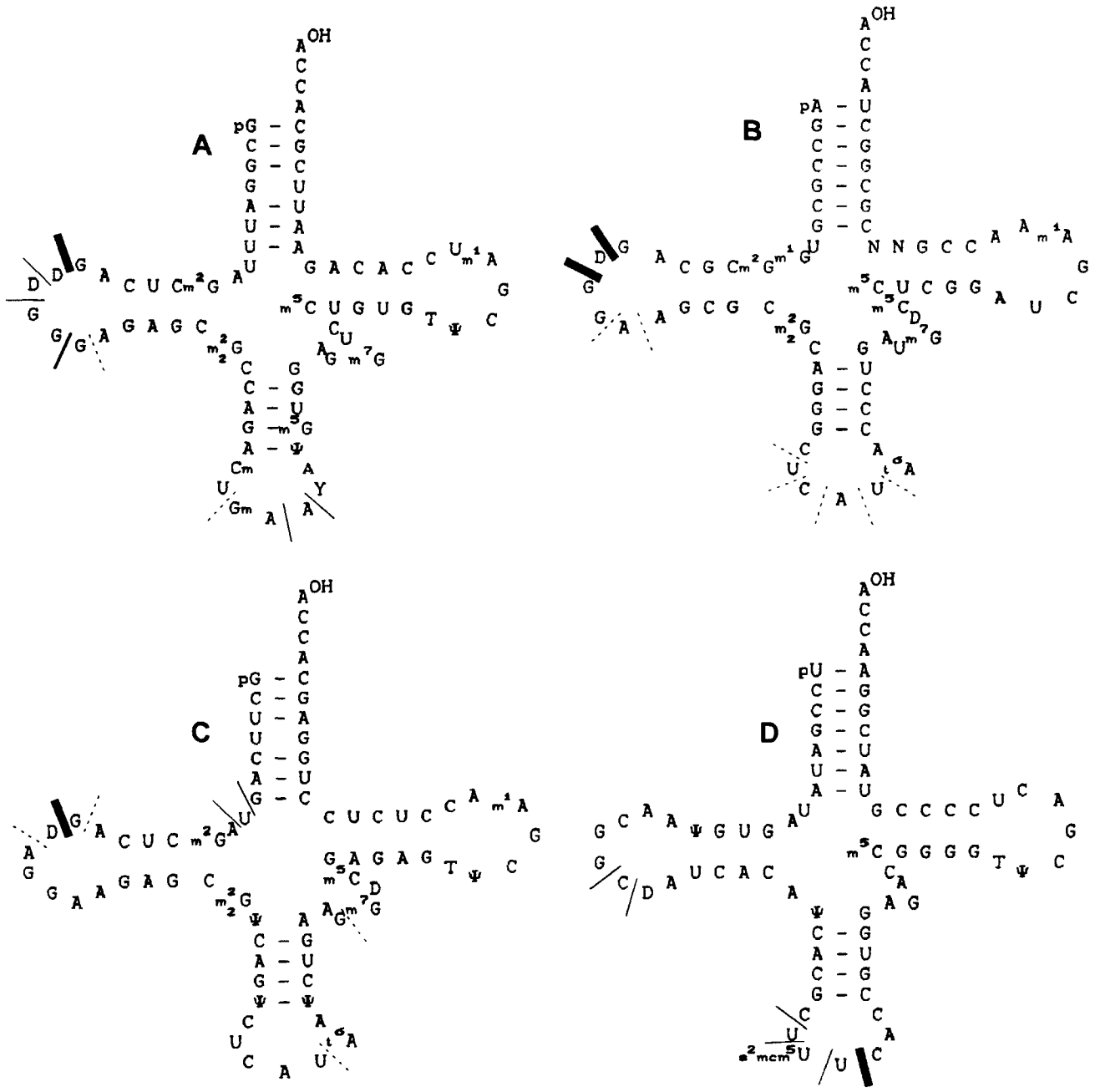

Fig. 3. Cloverleaf structure of yeast $tRNA^{Phe}$ (A), initiator $tRNA^{Met}$ (B), elongator $tRNA^{Met}$ (C) and $tRNA^{Glu}$ (D). The intensities of cleavages are correlated with thickness of the bars. Nucleotide sequence data are from Sprinzl et al. [41].

$tRNA^{Glu}$. In this tRNA very strong Mn(II) and Mg(II) cleavages occur in the anticodon loop at p36. This strong cleavage is accompanied by three weaker cuts at p33–p37 in case of Mn(II) ion-induced hydrolysis Fig. 2C). Also, only Mn(II) ions cut the D-loop of that tRNA at p19 and p20. In case of hydrolysis induced by Pb(II) and Eu(III) ions the main cleavage site in $tRNA^{Glu}$ occurs also at p36 of the anticodon loop but the efficiency of hydrolysis in standard conditions used for these ions [11,12] is much lower compared to that shown by Mn(II) and Mg(II) ions (data not shown).

3.6. *In vitro transcript representing yeast $tRNA^{Glu}$ anticodon arm*

Crystallographic and solution studies have shown that the anticodon arm is the region that does not interact with other parts of the tRNA molecule [30–32]. It was also shown that the anticodon loop of the isolated anticodon arm has an identical conformation as the anticodon loop of intact tRNA [33–34]. Thus the strong cleavage that occurs in the anticodon loop has to be induced by metal ion strongly bound somewhere within the loop region. To gain better insight into structural basis of this unusual reactivity of the anticodon loop we have prepared by in vitro transcription two RNA hairpin structures representing the yeast $tRNA^{Glu}$ anticodon arm and its variant with A37G base change.

To increase the yield of transcription and to strengthen the base pairing interaction within the stem region we added 3 extra G–C pairs and replaced G–ψ pair for G–C (Figs. 3,5). It was

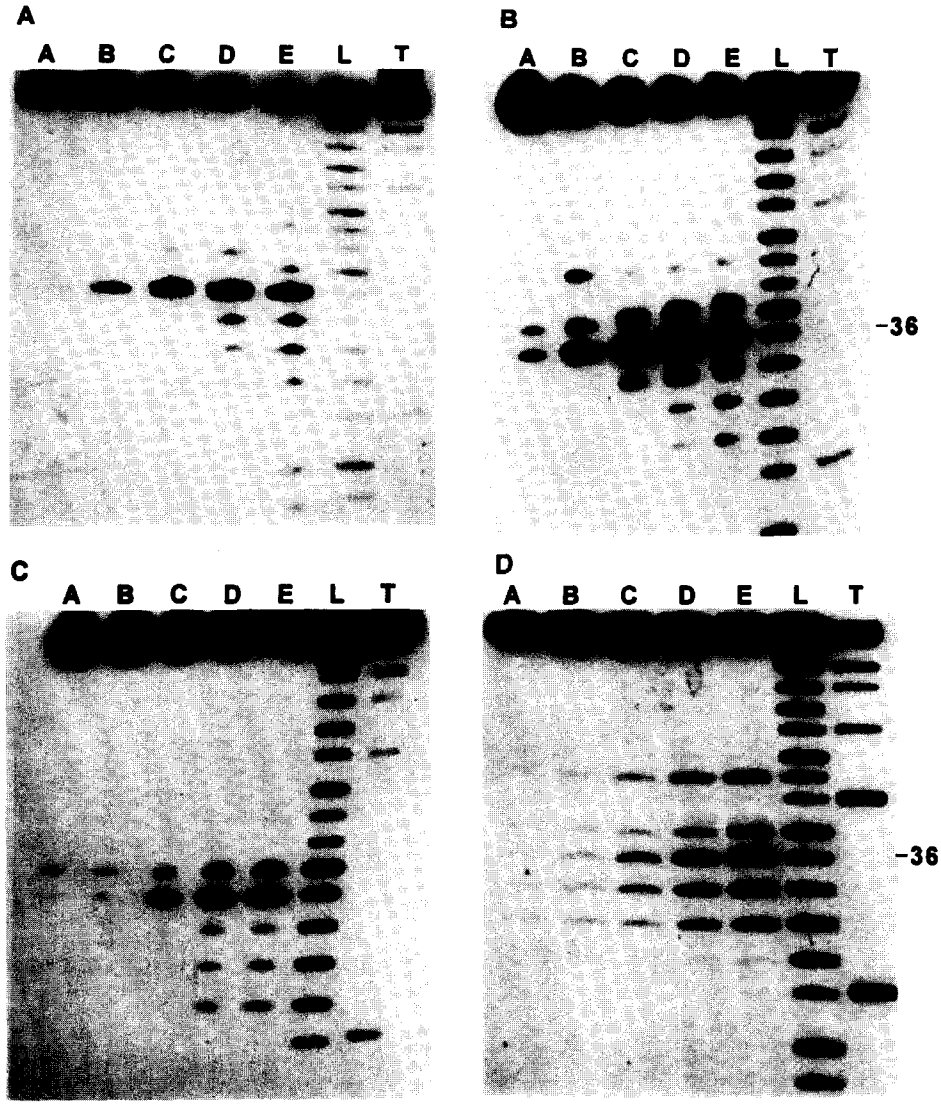

Fig. 4. Cleavage of yeast $tRNA^{Glu}$ anticodon arm transcript (A,B,C) and its A37G mutant (D) by Mg(II) (A), Mn (II) (B,D) and Pb(II) (C) ions. Reactions were performed at 37°C, for 12 h, at: B = 0.3, C = 1, D = 3, E = 10 mM concentration Mg(II) and Mn(II) ions. For the Pb(II) reaction, the following conditions were used: temperature 25°C, pH 7.2, time 20 min and Pb(II) concentration: B = 0.25, C = 0.5, D = 1, E = 2.5 mM. Lanes A = reaction control, lane L = formamide ladder, lane T = limited hydrolysis by RNase T_1. The numbers at the right correspond to the phosphates numbering in yeast $tRNA^{Phe}$ taken from Sprinzl et al. [41].

found that manganese and magnesium ions cut the anticodon loop of the transcript in a similar way as in intact $tRNA^{Glu}$. Comparing the efficiency of Mn(II)- and Mg(II)-induced hydrolysis (Fig. 4A,B), higher rate of cleavage is observed for Mn(II) ion. The Pb(II)-induced hydrolysis pattern is similar to that observed for Mn(II) and Mg(II) ions (Fig. 4C). Mutation of adenine-37 to guanine significantly reduces the specificity of the Mn(II)-induced hydrolysis (Figs. 4D,5) and the hydrolysis becomes also less efficient.

4. Discussion

We have chosen yeast $tRNA^{Phe}$ molecule as a primary model for our studies. The crystal and solution structure of this tRNA is well characterized and the location of strongly bound metal ions is well established. Using Mn(II) ions as a probe, a strong cleavage site in the D-loop has been found at p16. It means that somewhere in this region in tRNA structure in solution a strong manganese ion binding site is located. According to crystallographic data, in yeast $tRNA^{Phe}$ Mn(II) ion is bound directly to exocyclic nitrogen (N7) of G20 in the D-loop in a distance of 2 Å from the site where Mg(II) ion has been located [3]. The Mn(II) ion located at this site is most likely involved in cleavage of the D-loop of $tRNA^{Phe}$ in solution.

The cleavage effect observed in yeast elongator $tRNA^{Met}$ does not differ much from that found in $tRNA^{Phe}$. The location of the main cut at p16 is the same, however, its strength is higher in methionine-specific tRNA. Presumably the metal ion binding pocket formed by the interacting D- and T-loops has only slighly different structure in these two tRNAs. More different is the cleavage pattern observed in yeast initiator $tRNA^{Met}$.

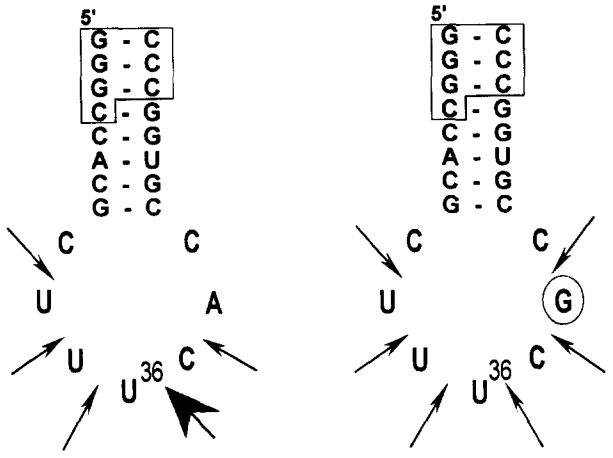

Fig. 5. Structures of yeast $tRNA^{Glu}$ anticodon arm transcript (left) and A37G mutant (right). The extra bases added to the stem are shown inside the box (see section 3). The arrows indicate Mn(II) ions cleavage sites. The numbering system is the same as in Fig. 4.

Two strong cuts occur in the D-loop at p16 and p17 while only one, at p16, was induced by Pb(II), Eu(III) and Mg(II) ions studied earlier [16]. This means that the environment of Mn(II) ion in the D-loop differs between yeast initiator and elongator $tRNA^{Met}$ and it is distinct in initiator tRNA from the location of other metal ions strongly bound to that region and involved in cleavage.

Entirely different pattern hydrolysis has been found in yeast $tRNA^{Glu}$. In case of this tRNA the strongest Mn(II), Mg(II), Pb(II) and Eu(III) cleavage appeared in the anticodon loop [35]. A similar high susceptibility of the anticodon loop to Mg(II) ion-induced cleavage has been described for *E. coli* $tRNA^{Glu}$ and its in vitro transcript [36]. In yeast $tRNA^{Glu}$ anticodon arm transcript, in which mcm^5s^2U34 hypermodification is absent, the efficiencies of Mn(II) and Mg(II) ion-induced hydrolysis are almost the same as in native tRNA molecule. Therefore the participation of the modified base in forming strong metal ion binding site within the loop can be excluded.

The loss of specificity of Mn(II)-induced hydrolysis in yeast $tRNA^{Glu}$ anticodon arm after A37 mutation to G (Fig. 4D) indicates that A37 participates in coordinating metal ion involved in cleavage. Several other mutants studied thus far show less prominent effect. The extensive mutagenesis of the anticodon loop of yeast $tRNA^{Glu}$ is in progress now in order to learn more about determinants of the cleavage strength and specificity. Some of the data presented in this paper show high similarity of cleavages induced by Mn(II) and Mg(II) ions. This is due to similar chemical properties of these ions [37]. Their hydrates show for example very close pK_a values: 10.6 and 11.4 for Mn(II) and Mg(II) ions, respectively [29]. They also show the same water coordination geometry. Owing to that manganese ions can replace magnesium ions in several biological systems. The examples are RNA catalysis reactions: *Tetrahymena* intron self-splicing [38], *E. coli* M1 RNA [39] and hammerhead domain ribozyme activity [40].

On the other hand, there are also remarkable differences in tRNA cleavage effects caused by manganese and magnesium ions. These differences fully justify using manganese ions as another RNA structure probing reagent. Besides the data presented in this paper also other studies from our laboratory have shown high usefulness of Mn(II) ions. For example yeast $tRNA^{Phe}$ U59C60 mutants the most significant differences in both the distribution and the efficiency of cleavages were observed using Mn(II) ions (D. Michalowski et al., in preparation). It has been shown that substitution of C60 by any other base strongly inhibits Mg(II)-induced hydrolysis. On the other hand, in case of Mn(II) ions the site of main cleavage is shifted but its efficiency remains the same or even is enhanced. These observations clearly indicate that Mg(II) and Mn(II) ions should be considered as distinct RNA structure probing reagents, capable of detecting subtly different features of folded RNA structures.

Acknowledgements: This work was supported by the Polish Committee for Scientific Research, Grant 6 P 203 026 04.

References

[1] Crothers, D.M. (1979) in: Transfer RNA: Structure, Properties and Recognition (Abelson, J., Schimmel, P.R. and Soll, D. eds.) pp. 163–178, Cold Spring Harbour Laboratory, Cold Spring Harbour, NY.
[2] Pan, T., Long, D.M. and Uhlenbeck, O.C., (1993) in: RNA World (Gesteland, R.F. and Atkins J.F. eds.) pp. 272–301, Cold Spring Harbour Laboratory Press, Cold Spring Harbour, NY.
[3] Jack, A., Ladner, J.E., Rhodes, D. and Klug, A. (1977) J. Mol. Biol. 111, 315–318.
[4] Hingerty, B., Brown, R.S. and Jack, A. (1978) J. Mol. Biol. 124, 523–524.
[5] Holbrook, S.R., Sussman, J.L., Warant, R.W., Church, G.M. and Kim, S.-H. (1977) Nucleic Acids Res. 4, 2811–2820.
[6] Quigley, G.J., Tetter, M.M. and Rich, A. (1978) Proc. Natl. Acad. Sci. USA 75, 64–68.
[7] Rubin, J.R. and Sundaralingam, M. (1983) J. Biomol. Struct. Dyn. 1, 639–646.
[8] Brown, J.R., Devan, J.C. and Klug, A. (1985) Biochemistry 24, 4785–4801.
[9] Rubin, J.R., Wang, J. and Sundaralingam, M. (1983) Biochim. Biophys. Acta 756, 111–118.
[10] Sampson, J.R., Sulivan, F.X., Behlen, L.S, DiRenzo, A.B. and Uhlenbeck, O.C. (1987) Cold Spring Harbour Symp. Quant. Biol. 52, 267–275.
[11] Krzyzosiak, W.J, Marciniec, T., Wiewiorowski, M., Romby, P., Ebel, J.P. and Giegie, R. (1988) Biochemistry 27, 5771–5777.
[12] Ciesiolka, J., Marciniec, T. and Krzyzosiak, W.J. (1989) Eur. J. Biochem. 182, 445–450.
[13] Marciniec, T., Ciesiołka, J., Wrzesinski, J. and Krzyzosiak, W.J. (1989) Acta Biochim. Polon. 36, 115–122.
[14] Labuda, D., Nicoghosian, K. and Cedergren, R. (1985) J. Biol. Chem. 260, 1103–1107.
[15] Marciniec, T., Ciesiołka, J., Wrzesinski, J. and Krzyzosiak, W.J. (1989) FEBS Lett. 243, 293–298.
[16] Ciesiołka, J., Wrzesinski J., Podkowinski, J., Gornicki, P. and Krzyzosiak, W.J. (1989) Eur. J. Biochem. 186, 71–77.
[17] Behlen, L.S., Sampson, J.R., DiRenzo, A.R. and Uhlenbeck, O.C. (1990) Biochemistry 29, 2515–2523.
[18] Michałowski, D., Wrzesinski, J., Ciesiołka, J. and Krzyzosiak W.J. (1995) submitted for publication.
[19] Pan, T., Gutell, R.R. and Uhlenbeck, O.C. (1991) Science 254, 1361–1364.
[20] Pan, T. and Uhlenbeck, O.C. (1992) Biochemistry 31, 3887–3895.
[21] Dichtl, B., Pan, T., DiRenzo, A.B. and Uhlenbeck, O.C. (1993) Nucleic Acids Res. 21, 531–535.
[22] Ciesiołka, J., Hardt, W.-D., Schlegl, J., Erdmann, V.A. and Hartmann, R.K. (1994) Eur. J. Biochem. 219, 49–56.
[23] Streicher, B., von Ahsen, U. and Schroeder, R. (1993) Nucleic Acids Res. 21, 311–317.
[24] Ciesiołka, J., Lorenz, S. and Erdmann, VA. (1992) Eur. J. Biochem. 204, 583–589 [25] Gornicki, P., Baudin, F., Romby, P., Wiewiorowski, M., Krzyzosiak, W.J., Ebel, J.P., Ehresmann, C. and Ehresmann, B. (1989) J. Biomol. Struct. Dyn. 6, 971–984.

[26] Ciesiołka, J., Lorenz, S. and Erdmann, V.A. (1992) Eur. J. Biochem. 204, 575–581.
[27] Milligan J.F., Groebe, D.R., Witherell, G.W. and Uhlenbeck, O.C. (1987) Nucleic Acids Res. 15, 8783–8798.
[28] Rordorf, B.F. and Kearns, D.R. (1976) Biopolymers 15, 1491–1504.
[29] Burgess, J. (1978) Metal Ions in Solution, pp 264–270, Horwood, Chichester, UK.
[30] Kim, S.-H. (1979) in: Transfer RNA: Structure, Properties and Recognition (Abelson, J., Schimmel, P.R. and Soll, D. eds.) pp. 83–99, Cold Spring Harbour Laboratory, Cold Spring Harbour, NY.
[31] Roy, S. and Redfield, A.G. (1983) Biochemistry 22, 1386–1390.
[32] Hilbers, C.W., Heerschap, A., Hasnoot, C.A.G. and Walters, J.A.L.I. (1983) J. Biomol. Struct. Dyn. 149, 649–655.
[33] Clore, G.M., Gronenborn, A.M., Piper, E.A., McLauglin, L.W., Graesner, E. and Van Boom, J.H. (1984) Biochem. J. 221, 737–751.
[34] Rose, S.J., Lowary, P.T. and Uhlenbeck, O.C, (1983) J.Mol. Biol. 167, 103–117.
[35] Wrzesinski, J. (1991) Ph.D. Thesis, Poznan University.
[36] Sylvers, L.A., Rogers, K.C., Shimizu, K.C., Othsuka, E. and Soll D. (1993) Biochemistry 32, 3836–3841.
[37] Fracisto da Silva, J.J.R. and Williams, R.J.P. (1991) The Biological Chemistry of the Elements, Clarendon Press, Oxford.
[38] Grosshans, C.A. and Cech, T.R. (1991) Biochemistry 28, 6888–6894.
[39] Kazakov, S. and Altman, S., (1991) Proc. Natl. Acad. Sci. USA 88, 9191–9197.
[40] Dahm, S.C. and Uhlenbeck, O.C. (1991) Biochemistry 30, 9364–9469.
[41] Sprinzl, M., Hartmann, T., Weber, J., Blank, J. and Zeidler, R. (1989) Nucleic Acids Res. 17, r1–r172.